BOLETIN LATINOAMERICANO Y DEL CARIBE DE PLANTAS MEDICINALES Y AROMÁTICAS
© / ISSN 0717 7917 / www.blacpma.ms-editions.cl

Articulo Original / Original Article

The relationships among Flory-Huggins specific interaction parameters, maximum amorphous capacity, and solid-state interactions of spray dried amorphous drug dispersions with conventional and novel pharmaceutical polymers

[Las relaciones entre los parámetros de interacción específicos de Flory-Huggins, la capacidad amorfa máxima y las interacciones en estado sólido de las dispersiones de fármacos amorfos secados por aspersión con polímeros farmacéuticos convencionales y nuevos]

Peter R. Freed[1] & David B. Lebo[1,2]

[1]Department of Pharmaceutical Sciences, School of Pharmacy, Temple University, Philadelphia, Pennsylvania, USA
[2]cGMP Services, School of Pharmacy, Temple University, Philadelphia, Pennsylvania, USA

Reviewed by:
Raul Vinet
Universidad de Valparaíso
Chile

Ali Parlar
Adiyaman University
Turkey

Correspondence
Peter R. **FREED**
peter.freed@temple.edu

Section Specific aspects

Received: 2 April 2021
Accepted: 2 May 2021
Accepted corrected: 8 July 2021
Published: 30 May 2022

Citation:
Freed PR, Lebo DB
The relationships among Flory-Huggins specific interaction parameters, maximum amorphous capacity, and solid-state interactions of spray dried amorphous drug dispersions with conventional and novel pharmaceutical polymers
Bol Latinoam Caribe Plant Med Aromat
21 (3): 389 - 403 (2022).
https://doi.org/10.37360/blacpma.22.21.3.23

Abstract: This study evaluated the specific interactions between drug and polymers in amorphous spray dried dispersions (SDDs). Four Biopharmaceutics Classification System (BCS) II class drugs were evaluated. Binary and ternary SDDs were manufactured with conventional polymers and arabinogalactan. Specific interaction parameters between drug and polymer were determined using theoretical calculations and DSC data. Analytical methods were used to evaluate solid and solution state interactions. Maximum amorphous content for each formulation was calculated using DSC. Flory-Huggins Specific Interaction Parameters were calculated. Negative specific parameters were associated with solid-state interactions and improved capacity of drug in the amorphous state. Ternary SDDs containing drug, polymer, and arabinogalactan displayed similar hydrogen bonding as was observed with binary SDDs. Solution-state interactions observed in binary systems may be used in tertiary systems to improve the amorphous drug capacity and improved dissolution compared to the binary. The resultant tertiary systems are an improvement over binary drug polymer systems.

Keywords: Amorphous dispersion; Flory-Huggins Model; Solubility enhancement; Solid state characterization; Bioavailability enhancement

Resumen: Este estudio evaluó las interacciones específicas entre el fármaco y los polímeros en dispersiones amorfas secadas por pulverización (SDD). Se evaluaron cuatro fármacos de clase II del Sistema de Clasificación Biofarmacéutica (BCS). Los SDD binarios y ternarios se fabricaron con polímeros convencionales y arabinogalactano. Los parámetros de interacción específicos entre el fármaco y el polímero se determinaron utilizando cálculos teóricos y datos de DSC. Se utilizaron métodos analíticos para evaluar las interacciones del estado sólido y de la solución. El contenido amorfo máximo para cada formulación se calculó usando DSC. Se calcularon los parámetros de interacción específicos de Flory-Huggins. Los parámetros específicos negativos se asociaron con interacciones en estado sólido y una capacidad mejorada del fármaco en el estado amorfo. Los SDD ternarios que contienen fármaco, polímero y arabinogalactano mostraron enlaces de hidrógeno similares a los observados con los SDD binarios. Las interacciones de estado de solución observadas en sistemas binarios pueden usarse en sistemas terciarios para mejorar la capacidad del fármaco amorfo y mejorar la disolución en comparación con el binario. Los sistemas terciarios resultantes son una mejora con respecto a los sistemas de polímeros de fármacos binarios.

Palabras clave: Dispersión amorfa; Modelo Flory-Huggins; Mejora de la solubilidad; Caracterización de estado sólido; Mejora de la biodisponibilidad

INTRODUCTION

Current pharmaceutical development tends to favor the selection of many more poorly water soluble active pharmaceutical ingredients (APIs) as candidates for oral solid dosage forms. These APIs tend to have low bioavailability without galenic manipulation. Formulation approaches are guided by whether an API is dissolution rate limited (DCS IIa) or solubility limited (DCS IIb) in biorelevant media (Butler & Dressman, 2010). Techniques to improve the dissolution rate include more traditional approaches such as micronization, excipient selection, and granulation with surfactant. Solubility limited APIs require more extensive modification to either alter or break the crystalline structure such as nanomilling, amorphous dispersion, or lipid formulation.

When the crystalline lattice has been eliminated for an amorphous form, the maintenance of this metastable state is a critical product attribute. The increased Gibbs free energy of the amorphous form results in a higher dissolution rate and improved kinetic solubility in comparison with the crystalline form, which is conversely results in a decrease in physical and chemical stability (Milne *et al*., 2015). Many excellent articles have investigated the similarities and interactions between API and excipients which may be predictive of physical stability. Polymeric inhibition of devitrification has been correlated to hydrogen bond interaction of molecular dispersion (Matsumoto & Zografi, 1999), and interactions between drug and polymer may also be correlated to physical stability of the systems (Forster *et al*., 2001).

The drugs selected for this research have been previously studied, characterized and formulated as amorphous dispersions. Ibuprofen amorphous solid dispersions have been prepared as a urea eutectic (You *et al*., 2014), PEG and poloxamer solid dispersion (Uddin *et al*., 2010), HPMC and poloxamer solid dispersion (Park *et al*., 2009), and microemulsion with surfactant (You *et al*., 2014). Ketoprofen amorphous solid dispersions have been formulated with PEG (Belyatskaya *et al*., 2019), povidone, copovidone, PVA (Di Martino *et al*., 2004; Rumondor *et al*., 2009; Chan *et al*., 2015), and Eudragit L100 (Yang *et al*., 2008). Nifedipine amorphous solid dispersions have been formulated with povidone, PEG, Gelucire (Wu *et al*., 2012), HPMC (Cilurzo *et al*., 2002), Eudragit RL, ethylcellulose (Huang *et al*., 2011), and Eudragit S100, HPMC (Ueda *et al*., 2018). Itraconazole amorphous solid dispersions have been formulated with HPMC (Janssen Pharmaceutica, 2020), povidone, copovidone (Verreck *et al*., 2003), Kollicoat IR, Eudragit E100 (Jennsens *et al*., 2010), PVP, HPMC-P, HPMC, methacrylate (Miller *et al*., 2008) and Soluplus (Zhang *et al*., 2013). The standard polymers selected in this study (HPMC, copovidone) have been successfully utilized for solid dispersions in the above referenced papers. A novel polymer, arabinogalactan, has not been cited in literature in combination with the selected drugs in either binary or ternary formulations. Arabinogalactan is of interest due to its branched structure, swellable nature, and rapid disintegration in aqueous media, and may increase dissolution rate of the solubilized drugs in SDD.

Correlations between Flory-Huggins specific interaction parameters and amorphous drug loading, solid state interactions, and solution state interactions between drug and polymer were observed. Utilizing the specific interaction parameter as a tool for prediction of maximum amorphous content can be a useful tool in drug product development to predict product performance and stability. It was found that a more negative specific interaction parameter correlates to higher drug loading of amorphous drug within the polymer system. A more negative specific interaction parameter also resulted in more observed solid and solution state interactions measured by FTIR and H-NMR.

MATERIALS AND METHODS

Materials

Ketoprofen (KTO), nifedipine (NIF), and itraconazole (ITRA) were purchased from TCI America (Portland, OR), and ibuprofen (IBU) was purchased from Fisher Scientific (Suwanee, GA). The four polymers chosen for this study were hydroxypropylmethylcellulose (HPMC) K3, hydroxypropylmethylcellulose (HPMC) E3, vinylpyrrolidone-vinyl acetate copolymer (copovidone) Kollidon VA64, and larch arabinogalactan. HPMC E3 and HPMC K3 were generously gifted from ShinEtsu (Niigata, JPN). Copovidone was purchased from BASF (Florham Park, NJ). Larch arabinogalactan was purchased from Lonza (Alpharetta, GA). Methanol and dichloromethane (ACS grade) were purchased from Fisher Scientific (Suwanee, GA). Chloroform-d with 1 v/v % TMS was purchased from Acros Organics (Geel, Belgium).

Preparation of physical mixture and spray dried dispersion

Spray dried solid dispersions (SDDs) were prepared in various ratios by dissolving the drug and polymer in a 1:1 v/v mixture of methanol:dichloromethane and spray dried using a Buchi B-290 spray dryer with inert loop. For formulations containing arabinogalactan, the arabinogalactan was dispersed in the drug and polymer solution and homogenized prior to spray drying. Operating parameters were set to: inlet temperature: 50-60°C, outlet temperature: 30-35°C, feed rate: 8-10 ml/min, aspirator: 100%. The outlet temperature was maintained below the theoretical glass transition temperature for the mixtures in order to avoid the semisolid transition of the material. Secondary drying was performed with a vacuum oven set to 30°C for 24 hours. All samples were stored desiccated and refrigerated prior to and after analysis. The compositions of the formulations and measured thermal properties in this study are seen in Table No. 1. The predicted glass transition temperature (T_g) was calculated using the Fox equation (Fox, 1956). Maximum amorphous content at onset melting point was calculated using the forthcoming Equation (2). Physical mixtures were prepared by mixing of weighed powders using a mortar and pestle.

Solid state characterization

The SDDs, raw materials, and physical mixtures were characterized using modulated differential scanning calorimetry (mDSC), Fourier transform infrared spectroscopy (FTIR), solution state proton nuclear magnetic resonance (^{1}H-NMR), scanning electron microscopy (SEM) and X-ray powder diffraction (XRPD). True density of all materials was measured using gas displacement pycnometry.

XRPD analysis

The diffractograms of samples were collected using a Rigaku MiniFlex 600 goniometer with a SC-70 detector. A sample size of approximately 50 mg was prepared in a sample holder and the samples were run at 40 kV and 15 mA. The samples were scanned from 3.00° to 60.00° 2θ at a rate of 10.0 degrees/minute. Data analysis was performed using MiniFlex+ software.

Thermal properties

The thermal properties of the spray dried dispersions, including onset of melting (T), drug melting point (T_m), heat of fusion (ΔH), and glass transition temperature (T_g) were measured using a TA Instruments Q2000 differential scanning calorimeter (mDSC). Glass transition temperatures were evaluated using high volume aluminum pans. Approximately 40 - 60 mg of material was packed into each hermetic high volume pan. Samples were heated from 20°C to 200°C with a ramp rate of 5°C/minute and modulation temperature amplitude of ±1.000°C. Reversible thermograms were collected to investigate glass transition temperatures. Non-reversible and heat flow thermograms were evaluated using standard aluminum pans. Approximately 5 - 10 mg of material was packed into a standard hermetic aluminum pan. Samples were heated from 0°C to 200°C with a ramp rate of 10°C/minute. The instrument was calibrated with indium before completing each sequence of tests. The melting point and heat of fusion of each drug was measured and used as a reference to calculate crystalline content and degree of crystallinity of each formulation at the onset of melting (Huang *et al*., 2011). All samples were run in duplicate.

$$\text{Crystalline content (\%, w/w)} = \frac{100\% \times \Delta H_{SD}}{\Delta H_{pure\ drug}} \quad (1)$$

$$\text{Maximum amorphous content} = \text{drug loading} - \text{crystalline content} \quad (2)$$

FTIR spectroscopy

Solid-state FTIR spectra were recorded over a wavenumber range of 4000 cm^{-1} to 500 cm^{-1} with a resolution of 0.9 cm^{-1} using a Nicolet 380 spectrometer. The spectra were analyzed using OMNIC Lite software, version 1.06.

Scanning Electron Microscopy

The morphology of the samples was evaluated using a JEOL JCM-6000 scanning electron microscope at an accelerating voltage of 10 kV. The samples were staged on a pedestal and coated with gold with a Cressington 108 sputtering system for 35 seconds and 30 mA.

^{1}H-NMR spectroscopy

Solution-state proton nuclear magnetic resonance spectra were recorded using a Bruker Ultrashield TM Plus 400 Mz NMR spectrometer. Approximately 5 mg of sample was dissolved into 0.9mL of deuterated chloroform with 1 v/v% TMS just before the analysis. The solution was filled into 5 mm NMR tubes and spectra recorded. The ^{1}H-NMR spectra were analyzed using TOPSPIN 21 software.

True density measurements

Skeletal density measurements were performed to calculate volume fraction in interaction parameter calculations. Measurements were taken with an AccuPyc II 1340 gas displacement pycnometer with nitrogen analysis gas at room temperature. Average densities were calculated from ten analyses per sample. All samples were tested in triplicate.

Calculation of drug – excipient interaction parameters

Flory-Huggins interaction parameters and calculated specific interaction parameters were calculated. Drug-excipient hydrophobic interactions can be characterized according to the below equation:

$$\chi_{1,2} = \frac{(\delta_1 - \delta_2)V_2}{RT} \quad (3)$$

Where T is the absolute temperature of the samples, R is the gas constant. δ_1 and δ_2 are the Hildebrand solubility parameters of the drug and excipients, calculated by group contribution method (van Krevelen, 1990). V is the molecular volume of the drug, calculated using molecular weight and molar volume based on the Hildebrand group contribution method.

The drug-polymer interaction parameter, which includes non-polar and specific interactions, was calculated using DSC data and Flory-Huggins theories (Huang *et al*., 2011). The drug solubility in polymer at onset melting temperature of each SDD was estimated using DSC and the true densities of the materials were determined using skeletal density pycnometry. The interaction parameter was calculated using Equation (4).

$$\chi_{2,1} = \frac{\left(\Delta H_2^{fuse}/R\right)\left(\left(1/T_m\right)-\left(1/T\right)\right)-\ln(\phi_2)-(1-\phi_2)}{(1-\phi_2)^2} \quad (4)$$

The interaction parameter calculation in Eq (4) used the following data: true densities of polymers in g/cm^3 [ρ_1 = 1.319 for HPMC E3, 1.346 for HPMC K3, 1.040 for copovidone, 1.049 for AG], measured using skeletal density pycnometry. True densities of drugs [ρ_2 = 1.116 for ibuprofen, 1.259 for ketoprofen, 1.371 for nifedipine, and 1.370 for itraconazole] were measured using skeletal density pycnometry.

A $X_{2,1}$ value of 0.5 or less indicates miscibility between the two components and a negative value indicates a high degree of specific interaction (Huang *et al*., 2011). The negative value also indicates a stronger drug-polymer interaction than drug-drug or polymer-polymer which predicts drug-polymer miscibility and drug loading capacity. Positive values indicate that drug-drug and polymer-polymer interactions are preferred over drug-polymer and may result in phase separation (Baghel *et al*., 2016).

RESULTS

X-ray powder diffraction

X-ray powder diffraction is a primary tool for evaluating the absence of crystallinity (Amorphous content) of the spray dried dispersion preparations. The preparation of drug and polymer solution in organic solvent, followed by the rapid drying and collection of spray dried powder may retain the amorphous nature of the drug substance, with inhibition of recrystallization by the dispersed polymer. Amorphous materials are metastable, therefore confirmation and maintenance of the formulation in an amorphous state is critical (Newman *et al*., 2008). As a reference, neat crystalline drug substances and each excipient were tested along with the spray dried dispersions.

Crystalline ibuprofen diffractograms were consistent with referenced materials, with characteristic peaks at 17.06, 20.43 and 22.65 2-theta (deg). Crystalline ketoprofen diffractograms were consistent with referenced materials, with characteristic peaks at 6.49, 18.48 and 22.89 2-theta (deg). Crystalline nifedipine diffractograms were consistent with referenced materials, with characteristic peaks at 8.21, 12.07, 16.39 and 24.72 2-theta (deg). Crystalline itraconazole diffractograms were consistent with referenced materials, with characteristic peaks at 14.76, 17.75, 20.65 and 23.74 2-theta (deg). Halo patterns were displayed for all SDDs, indicating the absence of crystalline material in the samples, in the exception of the 20% NIF: AG SDD sample. The selected diffractograms are displayed below in Figure No. 1. Each of the SDDs displayed in Figure No. 1 contain 40% drug.

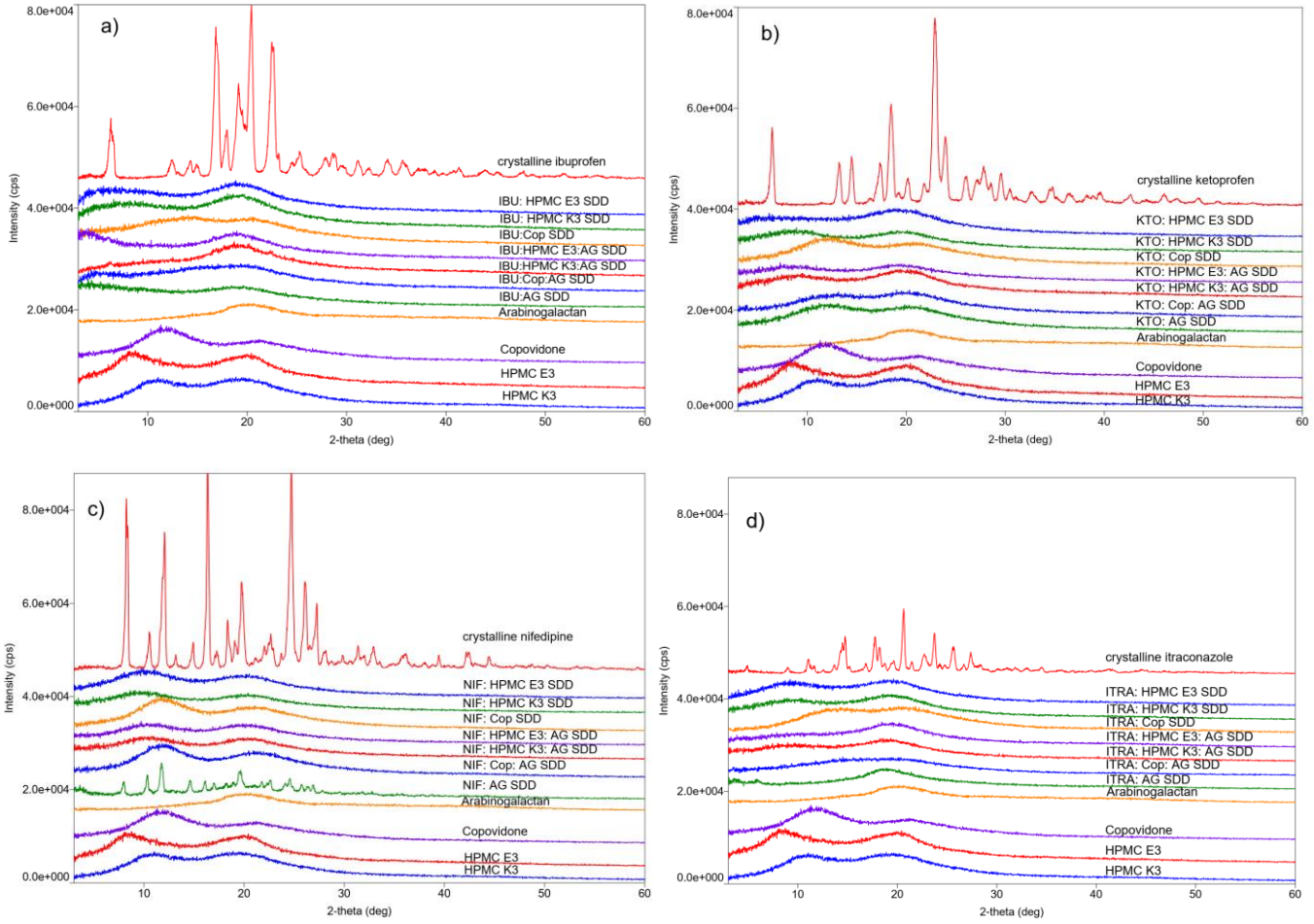

Figure No. 1
XRPD Spectra for a) ibuprofen and 40% ibuprofen SDDs, b) ketoprofen and 40% ketoprofen SDDs, c) nifedipine and 40% nifedipine SDDs, d) itraconazole and 40% itraconazole SDDs

DSC analysis

The spray dried dispersions and the starting materials were evaluated using modulated DSC. Glass transition temperatures were determined using reversible thermograms and reported alongside theoretical values calculated using Fox's Equation (Equation 5) in Table No. 1.

$$\frac{1}{T_g} = \frac{x_1}{T_{g1}} + \frac{1-x_1}{T_{g2}} \quad (5)$$

Enthalpy plots were generated and displayed in Figure No. 2 for SDD combinations of each drug and polymer with increasing drug content. True amorphous solid solutions of drug in polymer do not exhibit melting endotherms. Exothermic peaks observed for higher drug loads of nifedipine and itraconazole are indicative of cold crystallization of amorphous drug prior to melting (Aso *et al*., 2004).

Table No. 1
Glass transition temperatures for binary and ternary spray dried dispersions

Material	Drug Load (%w/w)	Tg Predicted (°C)	Tg Actual (°C)	Material	Drug Load (%w/w)	Tg Predicted (°C)	Tg Actual (°C)
Ibuprofen	-----	-----	-----	Nifedipine	-----	-----	-----
IBU:HPMC E3	20	95.2	96.9	NIF:HPMC E3	20	132.5	122.8
IBU:HPMC E3: AG	20	69.1	78.1	NIF:HPMC E3: AG	80	108.5	107.9
IBU:HPMC K3	20	95.2	85.0	NIF:HPMC K3	20	132.5	124.6
IBU:HPMC K3: AG	20	69.1	75.7	NIF:HPMC K3: AG	25	97.1	ND
IBU: Cop	20	52.7	ND	NIF: Cop	20	89.3	78.8
IBU:Cop: AG	20	59.2	50.1	NIF:Cop: AG	20	83.5	85.9
IBU: AG	20	46.4	55.1	NIF:AG	20	74.2	ND
Ketoprofen	-----	-----	-----	Itraconazole	-----	-----	-----
KTO: HPMC E3	10	136.7	130.9	ITRA:HPMC E3	20	136.3	137.5
KTO:HPMC E3: AG	10	112.2	105.8	ITRA:HPMC E3: AG	30	98.0	88.5
KTO: HPMC K3	10	136.7	137.3	ITRA:HPMC K3	20	136.3	149.2
KTO:HPMC K3: AG	10	112.2	111.4	ITRA:HPMC K3: AG	30	98.0	99.8
KTO: Cop	10	87.8	82.6	ITRA:Cop	20	92.3	82.0
KTO:Cop: AG	10	82.0	86.7	ITRA:Cop: AG	30	81.0	88.8
KTO: AG	10	71.0	72.0	ITRA:AG	20	76.9	72.3

FTIR Spectroscopy

The neat crystalline ketoprofen displayed shifts at 1654 and 1692 cm^{-1} characteristic of the C=O stretching of the carbonyl group and a triplet in the fingerprint region of 704 cm^{-1} (Blasi *et al*., 2007). Each spray dried sample prepared displayed a doublet in the fingerprint region with the absence of the peak at 704 cm-1 indicating the amorphous nature of the material. The spray dried dispersion KTO:HPMC K3 exhibits a shift at wavenumber 1658 cm^{-1}, spray dried dispersion KTO: HPMC E3 exhibits a shift at wavenumber 1655 cm^{-1}, and spray dried dispersion KTO:copovidone exhibits a shift at wavenumber 1656 cm^{-1}. The three shifts correspond to the carbonyl functional group of the ketoprofen molecule, and indication of potential hydrogen bonding with each polymer. The binary SDD comprised of ketoprofen and arabinogalactan does not differ from the peaks observed in the individual components, and the presence of the weak triple peak at 704 cm^{-1} indicates that the sample has some degree of crystallinity. Each ternary composition including drug, polymer, and arabinogalactan exhibits the same shift at wavenumber near the corresponding carbonyl wavenumber, indicating that inclusion of the arabinogalactan does not inhibit the hydrogen bonding between drug and polymer.

The neat crystalline ibuprofen displayed a characteristic shift at wavenumber 1708 cm^{-1}; assigned to the carbonyl stretching of self-associated ibuprofen dimers (Ghorab & Adeleye, 2001). The spray dried dispersion IBU:HPMC K3 exhibits a shift at wavenumber 1716 cm^{-1}, spray dried dispersion IBU: HPMC E3 exhibits an increased shift at wavenumber 1731 cm^{-1}, and spray dried dispersion IBU:copovidone exhibits a shift at wavenumber 1723 cm^{-1}. The binary SDD comprised of ibuprofen and arabinogalactan does not differ from the peaks observed in the individual components. The three binary shifts indicate disruption of the ibuprofen dimer and hydrogen bonding with polymer. The ternary composition containing drug, copovidone, and arabinogalactan exhibits the same carbonyl shift as the binary compositions. The ternary compositions containing drug, HPMC, arabinogalactan do not exhibit any shift and display similar peaks to those of

the individual components, indicating that the inclusion of arabinogalacatan has distrupted drug:polymer hydrogen bonding and that the ibuprofen dimer occurs in these combinations.

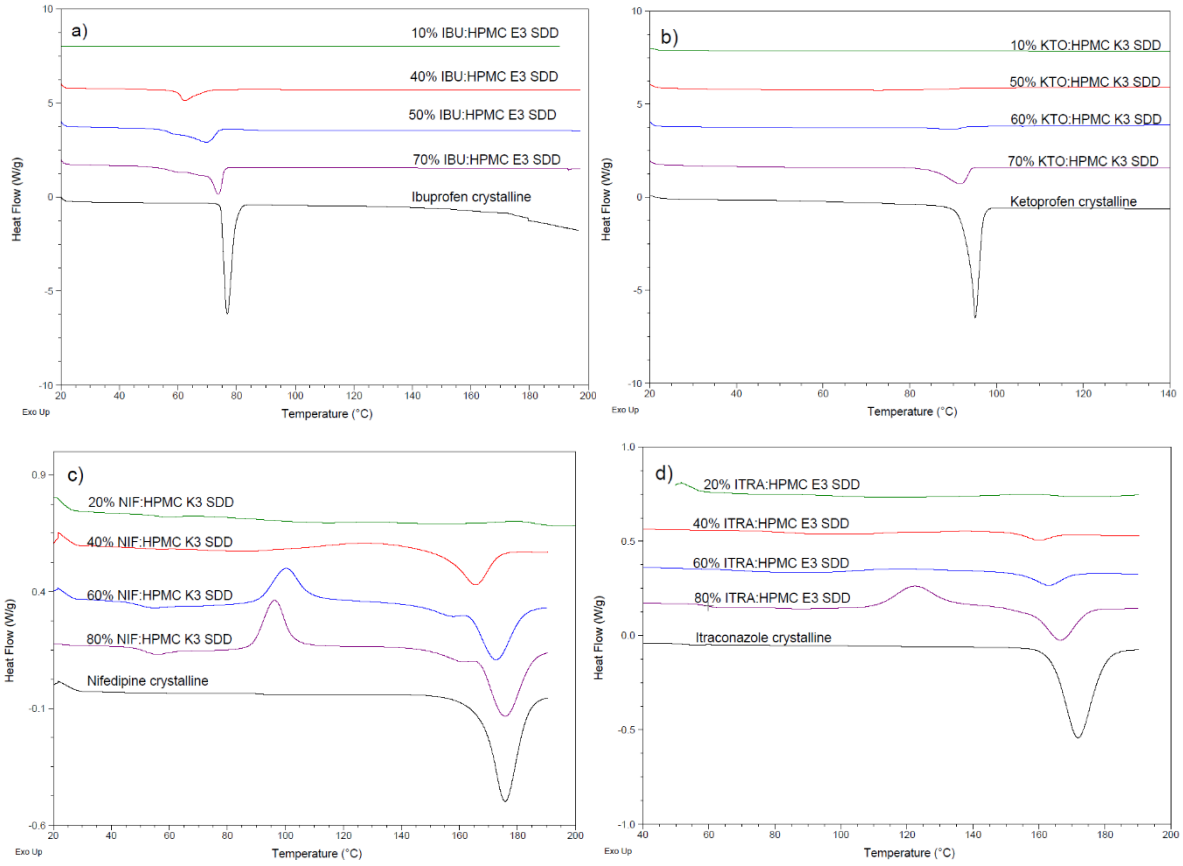

Figure No. 2
DSC thermograms for a) IBU:HPMC E3 SDDs, b) KTO:HPMC K3 SDDs, c) NIF:HPMC K3 SDDs d) ITRA:HPMC E3 SDDs

The neat crystalline nifedipine displayed two bands due to carbonyl groups at 1646 and 1677 cm^{-1} and an amide band at 3319 cm^{-1}. The spray dried dispersion NIF:HPMC K3 exhibits a shift at wavenumber 1680 cm^{-1}, spray dried dispersion NIF: HPMC E3 exhibits a shift at wavenumber 1697 cm^{-1}, and spray dried dispersion NIF:copovidone exhibits a shift at wavenumber 1658 cm^{-1}. The binary SDD comprised of nifedipine and arabinogalactan does not differ from the peaks observed in the individual components. The three shifts correspond to the carbonyl functional group of the nifedipine molecule, and indication of potential hydrogen bonding with each polymer. The ternary compositions containing drug, each polymer, and arabinogalactan each exhibit the same carbonyl shift as the binary compositions.

The neat crystalline itraconazole displays a characteristic peaks reported in literature as well as the peak at 1697 cm^{-1} that is attributed to the C=O group of the drug (Radzuan *et al*., 2010). The spray dried dispersion ITRA:HPMC K3 exhibits a shift at wavenumber 1228 cm^{-1}, spray dried dispersion ITRA: HPMC E3 exhibits shifts at wavenumbers 1227 and 1701 cm^{-1}, and spray dried dispersion ITRA:copovidone exhibits shifts at wavenumbers 1229, 1369, and 1730 cm^{-1}. Spray dried dispersion ITRA: AG exhibits shifts at wavenumbers 1227 and 1731 cm^{-1}. The shifts observed around 1226, 1369, and 1730 cm^{-1} correspond to the alcohol, alkane, and carbonyl functional groups of the itraconazole molecule, respectively. The ternary compositions containing drug, each polymer, and arabinogalactan each exhibit the same shifts as the binary compositions.

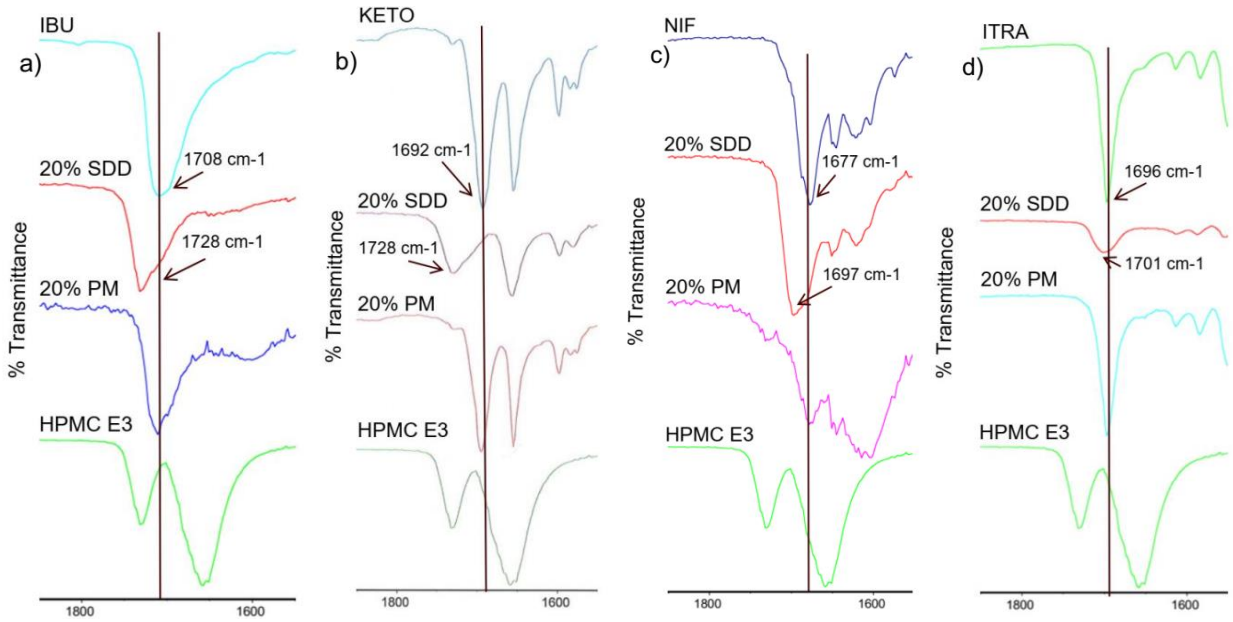

Figure No. 3
FTIR Spectra for carbonyl region of crystalline drugs, 20% spray dried dispersion, 20% physical mixtures, and HPMC E3 for a) ibuprofen, b)ketoprofen, c) nifedipine, d) itraconazole

^{1}H-NMR Spectroscopy

Solution-state ^{1}H-NMR of the individual components, physical mixtures, and spray dried dispersions was performed in order to determine whether the drug and polymer(s) interact or exhibit binding in solution. All solid dispersions evaluated contained 40% w/w drug. Deuterated chloroform with 1 v/v% TMS was utilized in order to dissolve the components shortly prior to analysis.

IBU:arabinogalactan spray dried dispersion exhibited three wavenumber shifts; at 7.4 ppm corresponding to the aromatic ring, at 2.4 ppm corresponding to the H3 proton on the skeletal backbone, and at 1.8 ppm corresponding to the H2 proton on the skeletal backbone.

The physical mixtures and spray dried dispersions of ketoprofen and HPMC E3,K3, and copovidone all exhibited the same shifts at 3.8 ppm corresponding to an aliphatic proton and at 7.6 ppm corresponding to an aromatic ring.

The physical mixtures and spray dried dispersions of nifedipine and HPMC E3, K3, and copovidone all exhibited the same shift at 1.5 ppm corresponding to the secondary amine and 5.7 ppm corresponding to an aromatic ring.

The physical mixtures of itraconazole and HPMC E3, K3, and copovidone all exhibited a shift at 1.6 ppm corresponding to an alkane proton. Spray dried dispersions of itraconazole and copovidone, and itraconazole and arabinogalactan exhibited the same shift at 1.6 ppm. Selected H-NMR profiles are displayed in Figure No. 4.

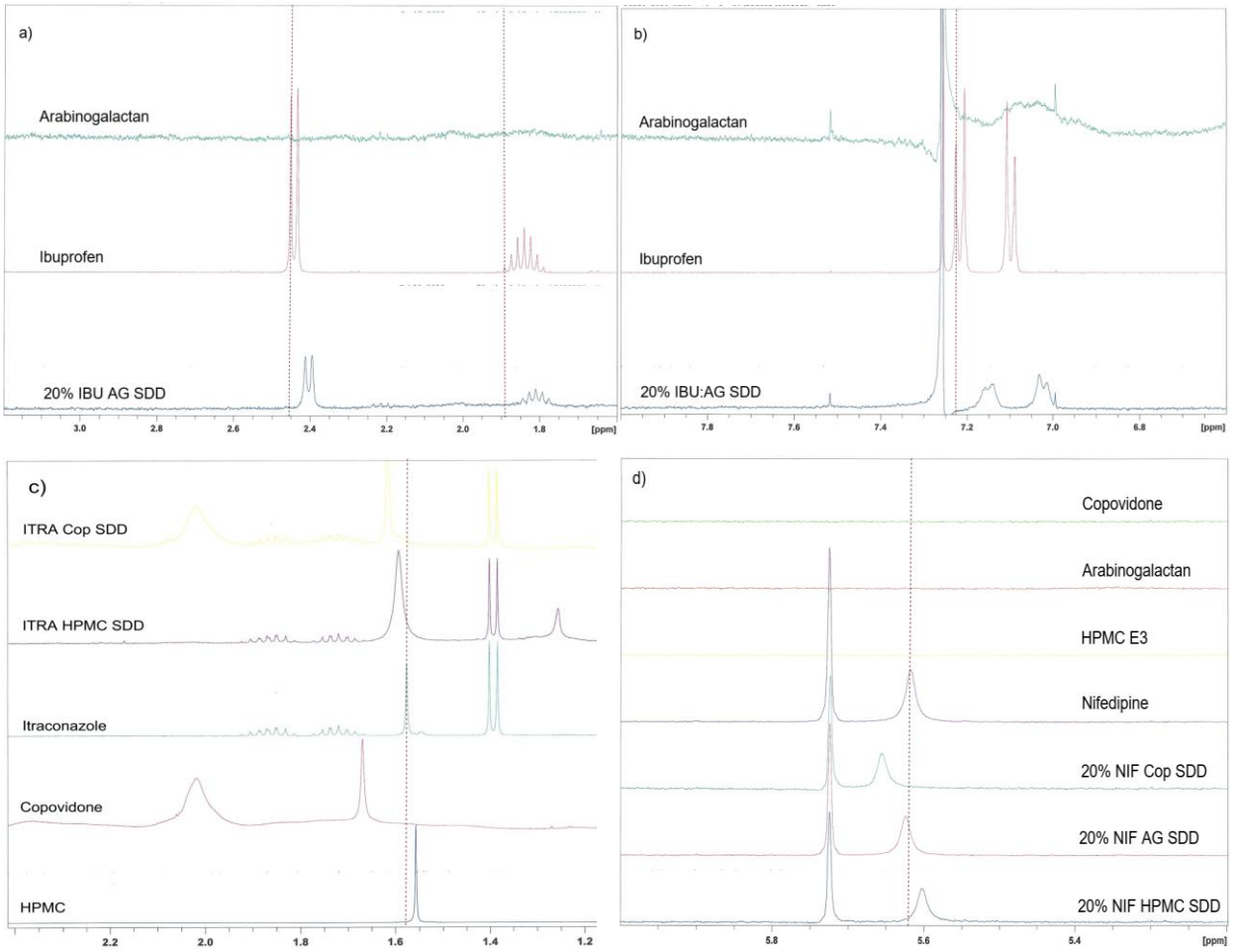

Figure No. 4
^{1}H-NMR spectra for a,b) Ibuprofen and IBU:AG SDD, c) itraconazole and ITRA SDDs, d) nifedipine and NIF SDDs

Scanning Electron Microscopy

A survey of the SDDs visibly confirmed the amorphous appearance of the spray dried drug:polymer particles, without emerging crystallization. Arabinogalactan, undissolved in the feed solution, can be observed as larger, irregular particles dispersed within the spray dried spheres.

DISCUSSION

In this study, many spray dried dispersions of drug and polymer(s) were investigated. Glass transition temperatures near theoretical values and XRPD analysis confirm that the powders are amorphous.

The FTIR characterization of ibuprofen was indicative of a positive interaction with both HPMC and copovidone. FTIR analysis of the binary spray dried formulations confirmed that the dimerization C=O peak prevalent in the crystalline form at 1708 cm-1 was replaced by a shifted peak at 1728 cm-1 that suggests hydrogen bonding between ibuprofen:HPMC and ibuprofen:copovidone. A similar phenomenon is reported in literature with ibuprofen:poloxamer solid dispersions (Ali *et al*., 2009). Such hydrogen bonding interactions are favorable for physical stability of the dispersions as well as maintenance of supersaturation upon dissolution of the drug product. Ternary spray dried dispersions containing arabinogalactan exhibited similar shifts, indicating that introduction of arabinogalactan did not disrupt hydrogen bonding between ibuprofen and either conventional polymer. Solution state interactions were not observed between ibuprofen:HPMC or ibuprofen:copovidone, however strong shifting was observed between ibuprofen:arabinogalactan. Shifts at 1.8, 2.4, 3.5, and 7.1 ppm for IBU-arabinogalactan were consistent

with hydrophobic interactions for B-cyclodextrin complexes (Ghorab & Adeyeye, 2001; Omari *et al*., 2009). These similarities suggest that the arabinogalactan polymer may form a tertiary drug-polymer complex perhaps due to coiling.

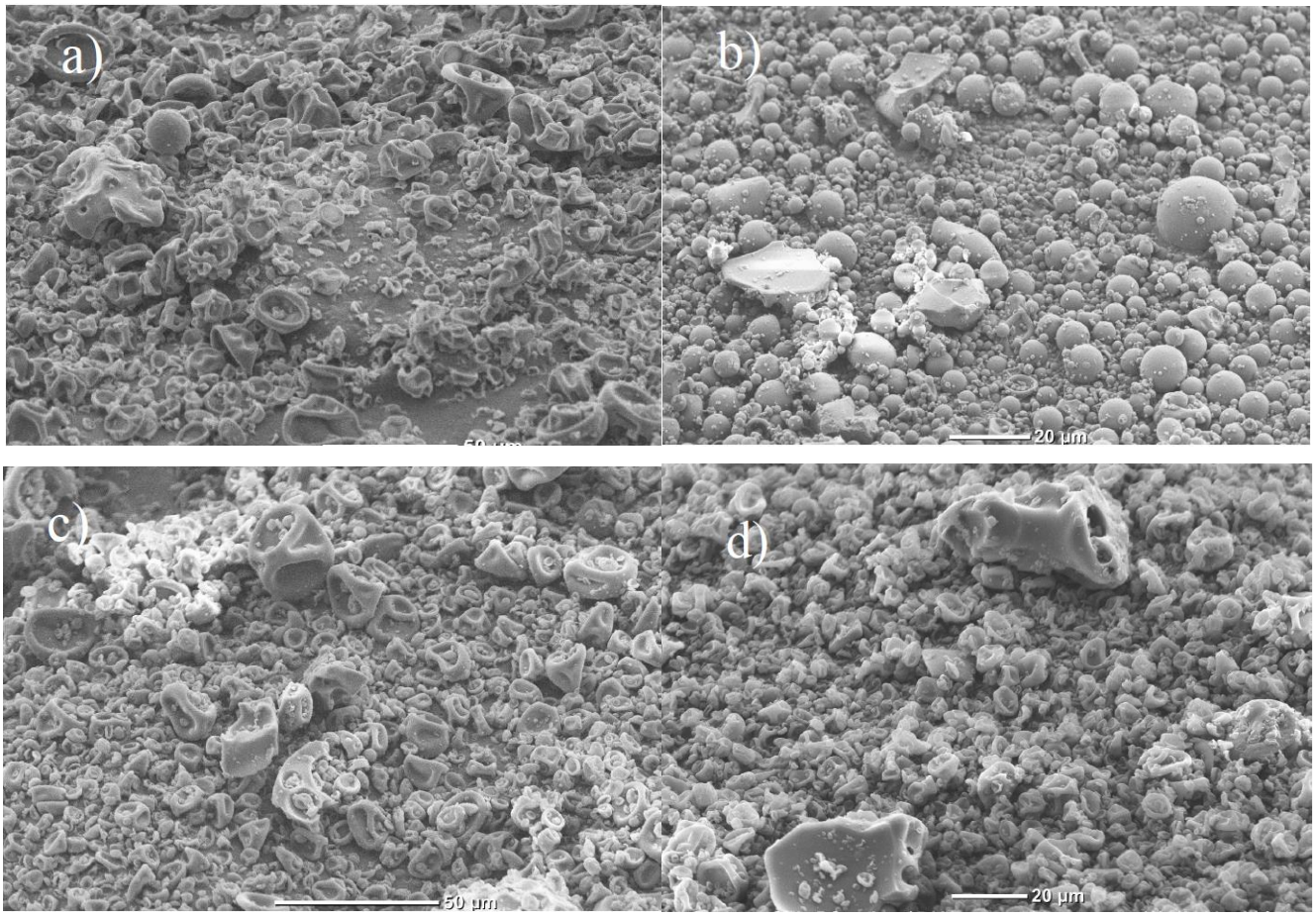

Figure No. 5
SEM images of a) IBU:HPMC E3:AG SDD, b) KTO:Cop:AG SDD, c) NIF:HPMC E3:AG SDD, d) ITRA:HPMC E3:AG SDD

The FTIR characterization of ketoprofen was, similarly to ibuprofen, indicative of hydrophobic interaction with HPMC and copovidone. The amorphous form of the spray dried samples with these polymers was confirmed with the absence of a triplet peak at 704 cm^{-1} that was present in the neat crystalline drug and physical mixtures (Park *et al*., 2009). Downshifted peaks were observed in the carbonyl moiety of the amorphous ketoprofen molecule as similarly observed in a KTO-copovidone system (Park *et al*., 2009). H-NMR Solution state characterization of ketoprofen and polymer showed an upfield chemical shift in the aromatic region of 7.4-7.8 ppm for keto-HPMC and keto-copovidone systems. This up field shift is indicative of a hydrophobic interaction, similar to the 'host-guest' type shifts observed in keto-βCD complexes (Marconi *et al*., 2010).

The FTIR characterization of nifedipine revealed a chemical shift of the ester carbonyl group from 1677 cm^{-1} in the neat crystalline to 1697 cm^{-1} in the amorphous dispersions of NIF:HPMC E3 and NIF:copovidone. Stretching of the amine groups was observed from 3319 cm^{-1} in the crystalline to 3333 cm^{-1} in the amorphous NIF:HPMC E3 and NIF:copovidone. Both ester carbonyl and amine stretching is indicative of hydrogen bonding between the amorphous drug and polymer (Huang *et al*.,

2007). Solution state interaction was observed as a chemical shift of the 4-H nifedipine proton at ~5.6 ppm with HPMC and copovidone. This interaction has not been cited previously in literature and is indicative of a possible solution state interaction between the drug and polymers.

The FTIR characterization of neat crystalline itraconazole indicated an intense C=O peak at 1696 cm^{-1} which broadened and shifted to ~1731 cm^{-1} for ITRA:HPMC and ITRA:copovidone SDDs. The resultant shift and peak broadening may be the result of hydrogen bonding (DiNunzio *et al*., 2008).

Calculated specific interaction parameters indicate interactions between the model drugs and polymers. An $X_{2,1}$ value below 0.5 is an indicator of miscibility between drug and polymer and a negative value indicates a high level of specific interactions such as hydrogen bonding (Lacoulonche *et al*., 1998).

DSC analysis of spray dried dispersions was used to calculate the maximum amorphous drug content in each polymer. The enthalpy peak measured and melting point was likewise utilized to calculate the Flory-Huggins specific interaction parameter, $X_{2,1}$. The results are displayed in Table No. 2.

Formulations with higher drug loading, although determined to be amorphous via XRPD, still displayed melting endotherms, which are indicative of a dispersion of amorphous drug rather that a true solid solution. Although a solid solution is ideal from a physical stability perspective, practical considerations such as dosage strength and size must be evaluated to strike the correct balance for a final dosage form. Due to this compromise, it is beneficial to choose an amorphous dispersion incorporating specific interactions with drug and polymer, while maximizing drug concentration as much as is practical and physically stable. The below Table No. 2 illustrates high amorphous content values with Ketoprofen, nifedipine, and itraconazole with HPMC and copovidone. Ibuprofen has lower maximum amorphous contents near 20% in each polymer, likely due to the low melting point of the drug. Each drug has lower maximum amorphous contents in arabinogalactan. Negative specific interaction parameters calculated for ibuprofen correlate to observed FTIR shifts indicative of hydrogen bonding. Negative interaction parameters for nifedipine, ketoprofen, and itraconazole dispersions correlate to both FTIR and HNMR shifts. An anomaly is the positive interaction parameter for Keto:copovidone with both FTIR and HNMR shifts observed. The relationships between the F-H interaction parameter, solid state interaction, solution state interaction, and maximum amorphous content are displayed in Table No. 2.

The arabinogalactan polymer, which was undissolved in the spray drying feed solution, did not disrupt the hydrogen bonding observed that had been observed in many of the ternary mixtures in the solid state. The addition of arabinogalactan may be beneficial in dissolution rate enhancement of the solid form due its branched structure and swellable characteristics, while the hydrogen bonding between drug and polymer is maintained, potentially leading to enhanced stability and maintenance of the supersaturated state of drug in solution.

CONCLUSION

This study combined of solid-state methods, solution state methods, and in silico calculations to correlate the maximum amorphous drug content, solid state, and solution state interactions to the Flory Huggins interaction parameter in amorphous drug dispersions. Many previous studies have relied on calculated solubility parameters and the hydrophobic F-H interaction drug-parameter (Equation 3) to predict miscibility, drug loading, and solid-state interactions, however these in silico calculations lack precision in that the criteria for miscibility is generally stated as $\Delta\delta$ <7 MPa-1 (Forster *et al*., 2001), whereas the majority of calculated Hildebrand solubility parameter values are within this range. This is the limitation of using total Hildebrand solubility parameters in general, it may be beneficial to investigate integration of the three individual Hansen parameters into these equations or to evaluate specificity of individual Hansen terms to predict solid state or solution state interaction. The F-H specific interaction parameter incorporates in silico group contribution calculations paired with experimental data to calculate a more predictive indicator of miscibility and extent of drug loading. The limitations of this approach are the previously mentioned Hildebrand solubility parameter imprecision and the variance in the thermal data analysis. The specific interaction parameter calculation incorporates heat of fusion as well as melting point of an amorphous sample, but amorphous dispersions that are completely miscible do not exhibit a melting point event, to obtain the melting point data, sample must be manufactured and tested that are amorphous but not entirely miscible. This exercise, however, allows the researcher to push the limit of amorphous drug loading within each

polymer and concludes with an optimized maximum amorphous content value and a general understanding of the 'safe' amorphous dispersion drug loading levels for each drug:polymer ratio. FH interaction factors and the data can be utilized to determine a maximal drug load but a positive interaction factor does not mean that an ASD does not form using the polymer and the drug. ASD can occur without a significant polymer interaction however the drug loading is low in these dispersions.

Table No. 2
Correlations between F-H Interaction Parameter, FTIR shift, H-NMR shift, and maximum amorphous content

Material	Drug Load (%w/w)	Enthalpy peak area (J/g)	Max. Amorphous Content (%w/w)	Calculated Flory-Huggins interaction parameter (χ_{FH})	FTIR Shift	H-NMR Shift	Amorphous
Ibuprofen	n/a	132.7	n/a	n/a	n/a	n/a	-
IBU:HPMC E3	50	43.61	17.1	-0.089	+	-	+
IBU:HPMC K3	20	0.36	19.7	-0.174	+	-	+
IBU: Cop	60	50.8	21.8	-0.655	+	-	+
IBU: AG	20	ND	20[1]	1.240	-	+	+
Ketoprofen	n/a	112.8	n/a	n/a	n/a	n/a	-
KTO: HPMC E3	60	0.73	59.4	-1.460	+	+	+
KTO: HPMC K3	60	4.6	55.9	-1.150	+	+	+
KTO: Cop	20	ND	20[1]	0.906	+	+	+
KTO: AG	20	8.42	12.5	1.104	-	-	+
Nifedipine	n/a	115	n/a	n/a	n/a	n/a	-
NIF:HPMC E3	60	21.56	41.3	-0.190	+	+	+
NIF:HPMC K3	60	26.79	36.7	0.283	-	+	+
NIF: Cop	60	4.19	56.4	-1.638	+	+	+
NIF:AG	40	62	26.5	0.870	-	-	-
Itraconazole	n/a	91.4	n/a	n/a	n/a	n/a	-
ITRA:HPMC E3	60	8.057	51.2	-1.511	+	+	+
ITRA:HPMC K3	60	11.83	47.1	-1.114	+	+	+
ITRA:Cop	60	18.43	39.8	-1.117	+	+	+
ITRA:AG	40	37.8	18.6	0.343	-	-	+

A correlation has been illustrated in Figure 6 between the Flory-Huggins drug-polymer specific interaction parameter ($X_{2,1}$) and drug loading, defined as maximum amorphous content. This correlation is useful to screen polymers to rank-order potential drug loading based on the specific interaction parameters that are generated experimentally. Table No. 2 illustrates the relationship that was determined between specific interaction parameters and solid state and solution state interactions observed. A novel polymer, arabinogalactose, was incorporated into tertiary formulations to investigate whether this disruption would affect solid state interactions. It was determined that arabinogalactan did not disrupt any hydrogen bonding between drug and polymers observed in the binary mixtures, suggesting that the tertiary dispersons will exhibit similar characteristics and physical stability. These tertiary formulations may be beneficial because arabinogalactan is a highly soluble, swellable polymer that may aid dissolution of amorphous dispersions.

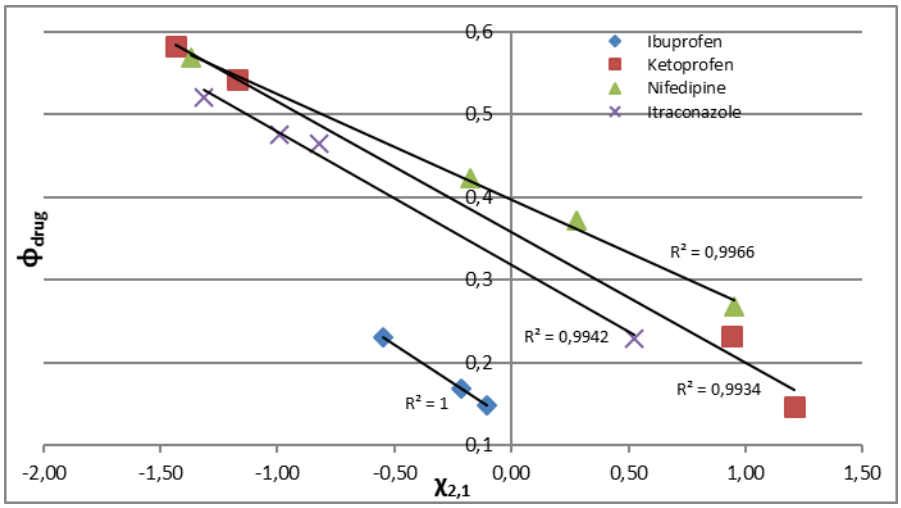

Figure No. 6
The relationship between the specific interaction parameter and maximum amorphous content

REFERENCES

Ali W, Williams AC, Rawlinson CF. 2009. Stochiometrically governed molecular interactions in drug: Poloxamer solid dispersions. **Int J Pharm** 391: 162 - 168. **https://doi.org/10.1016/j.ijpharm.2010.03.014**

Aso Y, Yoshioka S, Kojima S. 2004. Molecular mobility-based estimation of the crystallization rates of amorphous nifedipine and phenobarbital in poly(vinylpyrrolidone) solid dispersions. **J Pharm Sci** 93: 384 - 391. **https://doi.org/10.1002/jps.10526**

Baghel S, Cathcart H, O'Reilly NJ. 2016. Polymeric amorphous solid dispersions: a review of amorphization, crystallization, stabilization, solid-state characterization, and aqueous solubilization of biopharmaceutical classification system class II drugs. **J Pharm Sci** 105: 2527 - 2544. **https://doi.org/10.1002/chin.201642262**

Belyatskaya AV, Krasnyuk Jr II, Krasnyik II, Stepanova OI, Kosheleva TM, Kudinova TP, Vorob'ev AN, Maryanyan MM. 2019. Dissolution of ketoprofen form poly(ethylene glycol) solid dispersions. **Pharm Chem J** 52: 1001 - 1006. **https://doi.org/10.1007/s11094-019-01941-0**

Blasi P, Schoubben A, Giovagnoli S, Perioli L, Ricci M, Rossi C. 2007. Ketoprofen poly(lactide-co-glycolide) physical interaction. **AAPS PharmSciTech** 37: E78 - E85. **https://doi.org/10.1208/pt0802037**

Butler JM, Dressman JB. 2010. The developability classification system: application of biopharmaceutics concepts to formulation development. **J Pharm Sci** 99: 4940 - 4954. **https://doi.org/10.1002/jps.22217**

Chan SY, Chung YY, Cheah XZ, Yen-Ling E, Quah TJ. 2015. The characterization and dissolution performances of spray dried solid dispersion of ketoprofen in hydrophilic carriers. **Asian J Pharm Sci** 10: 372 - 385. **https://doi.org/10.1016/j.ajps.2015.04.003**

Cilurzo F, Minghetti P, Casiraghi A, Montanari L. 2002. Characterization of nifedipine solid dispersions. **Int J Pharm** 242: 313 - 317. **https://doi.org/10.1016/s0378-5173(02)00173-4**

Di Martino P, Joiris E, Gobetto R, Masic A, Palmieri GF, Martelli S. 2004. Ketoprofen-poly(vinylpyrrolidone) physical interaction. **J Cryst Growth** 265: 302 - 308. **https://doi.org/10.1016/j.jcrysgro.2004.02.023**

DiNunzio JC, Miller DA, Yang W, McGinity JW, Williams RO. 2008. Amorphous compositions using concentrations enhancing polymers for improved bioavailability of itraconazole. **Mol Pharmaceutics** 5: 968 - 980. **https://doi.org/10.1021/mp800042d**

Forster A, Hempenstall J, Rades T. 2001. Characterization of glass solutions of poorly water-soluble drug produced by melt extrusion with hydrophilic amorphous polymer. **J Pharm Pharmacol** 53: 303 - 315. **https://doi.org/10.1211/0022357011775532**

Fox TG. 1956. Influence of diluent and of copolymer composition on the glass temperature of a polymer system. **Bull Amer Phy Soc** 1: 123.

Ghorab MK, Adeyeye MC. 2001. Elucidation of solution state complexation in wet-granulated oven-dried

ibuprofen and β-cyclodextrin: FT-IR and ^{1}H-NMR studies. **Pharm Dev Technol** 6: 315 - 324. **https://doi.org/10.1081/pdt-100002612**

Huang J, Wigent RJ, Schwartz JB. 2007. Drug-polymer interaction and its significance on the physical stability of nifedipine amorphous dispersion in microparticles of an ammonio methacrylate copolymer and ethylcellulose binary blend. **J Pharm Sci** 97: 251 – 262. **https://doi.org/10.1002/jps.21072**

Huang J, Li Y, Wigent RJ, Malick WA, Sandhu HK, Singhal D, Shah NH. 2011. Interplay of formulation and process methodology on the extent of nifedipine molecular dispersion in polymers. **Int J Pharm** 420: 59 - 67. **https://doi.org/10.1016/j.ijpharm.2011.08.021**

Jannsens S, De Zeure A, Paudel A, Humbeeck JV, Rombaut P, Van den Mooter G. 2010. Influence of preparation methods on solid state supersaturation of amorphous solid dispersions: A case study with itraconazole and Eudragit E100. **Pharm Res** 27: 775 - 785. **https://doi.org/10.1007/s11095-010-0069-y**

Janssen Pharmaceutica, 2020. **Sporanox**. Package Insert.

Lacoulonche F, Chauvet A, Masse J, Egea MA, Garcia ML. 1998. An investigation of FB interactions with poly(ethylene glycol) 6000, poly(ethylene glycol) 4000, and poly-E-caporlactone by thermoanalytical and spectroscopic methods and modeling. **J Pharm Sci** 87: 543 - 551. **https://doi.org/10.1021/js970443+**

Marconi G, Mezzina E, Manet I, Manoli F, Zambelli B, Monti S. 2010. Steroselective interaction of ketoprofen enantiomers with β-cyclodextrin: ground state binding and photochemistry. **Photochem Photobiol Sci** 10: 48 - 59. **https://doi.org/10.1039/c0pp00262c**

Matsumoto T, Zografi G. 1999. Physical properties of solid molecular dispersions of indomethacin with poly (vinylpyrrolidone) and poly (vinylpyrrolidone-co-vinyl-acetate) in relation to indomethacin crystallization. **Pharm Res** 16: 1722 - 1728.

Miller DA, DiNunzio JC, Yang, W, McGinity JW, Williams RO. 2008. Enhanced *in vivo* absorption of itraconazole via stabilization of supersaturation following acidic-to-neutral pH transition. **Drug Dev Ind Pharm** 34: 890 - 902. **https://doi.org/10.1080/03639040801929273**

Milne M, Liebenberg W, Aucamp M. 2015. The stabilization of amorphous zopiclone in an amorphous solid dispersion. **AAPS PharmSciTech** 16: 1190 - 1202. **https://doi.org/10.1208/s12249-015-0302-4**

Newman A, Engers D, Bates S, Ivanisevic I, Kelly RC, Zografi G. 2008. Characterization of amorhous API:polymer mixtures using X-ray powder diffraction. **J Pharm Sci** 97: 4840 - 4856. **https://doi.org/10.1002/jps.21352**

Omari A, Mahmoud M, Daraghmeh NH, El-Barghouthi MI, Zughul MB, Chowdhry BZ, Leharne SA, Badwana AA. 2009. Novel inclusion of ibuprofen tromethamine with cyclodextrins: Physico-chemical characterization. **J Pharm Biomed** 50: 449 - 458. **https://doi.org/10.1016/j.jpba.2009.05.031**

Park YJ, Kwon R, Quan QZ, Oh DH, Kim JO, Hwang MR, Koo YB, Woo JS, Yong CS, Choi HG. 2009. Development of novel ibuprofen-loaded solid dispersion with improved bioavailability using aqueous solution. **Arch Pharm Res** 32: 767 - 772. **https://doi.org/10.1007/s12272-009-1516-3**

Radzuan R, Majeed ABA, Hamzah MK. 2010. Verified *in vitro* characteristics of ketoconazole and itraconazole nanoparticulates in wet-nanomilling. **IEEE Symposium on Industrial Electronics and Applications https://doi.org/10.1109/isiea.2010.5679431**

Rumondor ACF, Ivanisevic I, Bates S, Alonzo DE, Taylor LS. 2009. Evaluation of drug-polymer miscibility in amorphous solid dispersion systems. **Pharm Res** 26: 2523 - 2534. **https://doi.org/10.1007/s11095-009-9970-7**

Uddin R, Saffoon N, Huda NH, Jhanker YM. 2010. Effect of water soluble polymers on dissolution enhancement of ibuprofen solid dispersion prepared by fusion method. **Stamford J Pharm Sci** 3: 63 - 67. **https://doi.org/10.3329/sjps.v3i1.6801**

Ueda K, Yamazoe C, Yasuda Y, Higashi K, Kawakami K, Moribe K. 2018. Mechanism of enhanced nifedipine dissolution b polymer-blended solid dispersion through molecular-level characterization. **Mol Pharm** 15: 4099 - 4109. **https://doi.org/10.1021/acs.molpharmaceut.8b00523**

Van Krevelen, DW. 1990. **Properties of polymers.** Elsevier, Amsterdam, The Netherland.

Verreck G, Chun I, Rosenblatt J, Peeters J, Dijck AV, Mensch J, Noppe M, Brewster ME. 2003. Incorporation of drugs in an amorphous state into electrospun nanofibers composed of a water-insoluble, nonbiodegradable polymer. **J Control Release** 92: 349 - 360. **https://doi.org/10.1016/s0168-3659(03)00342-0**

Wu JY, Ho HO, Chen YC, Chen CC, Sheu MT. 2012. Thermal analysis and dissolution characteristics of nifedipine solid dispersions. **J Food Drug Anal** 20: 27 - 33.

Yang R, Wang Y, Zheng X, Meng J, Tang X, Zhang X. 2008. Preparation and evaluation of ketoprofen hot-melt extruded enteric and sustained-release tablets. **Drug Dev Ind Pharm** 34: 83 - 89. **https://doi.org/10.1080/03639040701580572**

You X, Xing Q, Tou J, Song W, Zeng Y, Hua H. 2014. Optimizing surfactant content to improve oral bioavailability of ibuprofen in microemulsions: just enough or more than enough? **Int J Pharm** 471: 276 - 284. **https://doi.org/10.1016/j.ijpharm.2014.05.031**

Zhang K, Yu H, Luo Q, Yang S, Lin X, Zhang Y, Tian B, Tang X. 2013. Increased dissolution and oral absoption of itraconazole/Soluplus extrudate compared with itraconazole nanosuspension. **Eur J Pharm Biopharm** 85: 1285 - 1292. **https://doi.org/10.1016/j.ejpb.2013.03.002**